# Comparison of Constitutive Models for Triaxially Loaded Concrete
## Comparaison de modèles de comportement du béton sous charge triaxiale
## Vergleich konstitutiver Modelle für Beton unter dreiachsialer Belastung

**J. EBERHARDSTEINER**
University Assistant
Technical Univ.
Vienna, Austria

**G. MESCHKE**
Research Assistant
Technical Univ.
Vienna, Austria

**H.A. MANG**
Professor
Technical Univ.
Vienna, Austria
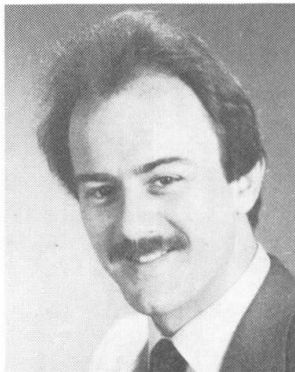
Josef Eberhardsteiner, born 1957, graduated as Dipl.-Ing. (Civil Engineer) from TU-Vienna in 1983. Since then he has been a University Assistant at the Institute of Strength of Materials at TU-Vienna.

Günther Meschke, born 1958, graduated as Dipl.-Ing. (Civil Engineer) from TU-Vienna in 1983. Since then he has been a Research Assistant at the Institute of Strength of Materials at TU-Vienna.

Herbert A. Mang, born 1942, graduated as Dr.techn. (1970), from TU-Vienna, Ph.D. (1974) from Texas Tech. University; University Assistant (1967), Professor (1983), both at TU-Vienna; Corresponding Member of the Austrian Academy of Sciences (1985).

## SUMMARY

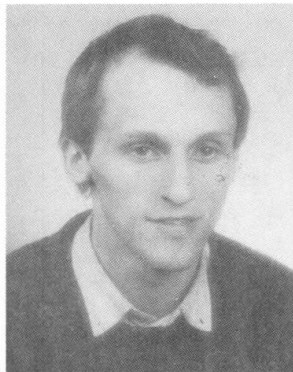After a description of four triaxial constitutive models for concrete, based on different mechanical concepts, a comparative evaluation is carried out. One of the models is a new hypoplastic model. Shortcomings of some models, occurring in case of non-monotonic load histories, are eliminated by adequate modifications. Generally, there is a good agreement between model predictions and test results.

## RÉSUMÉ

Une présentation de quatre modèles triaxiaux de comportement du béton sur la base des différentes théories mécaniques est suivie d'une évaluation comparative. Un des modèles est une nouvelle formulation hypoplastique. Quelques modèles présentent des défauts – lors de cas de charges non-monotones – lesquels sont éliminés par des modifications appropriées. Généralement, les résultats du modèle correspondent bien avec des résultats expérimentaux.

## ZUSAMMENFASSUNG

Vier auf verschiedenen mechanischen Konzepten beruhenden dreiachsiale konstitutive Modelle für Beton werden beschrieben und einer vergleichenden Wertung unterzogen. Eines dieser Modelle ist ein neues hypoplastisches Modell. Mängel einzelner Modelle, die bei nichtmonotonen Lastgeschichten auftreten, werden durch geeignete Modifikationen beseitigt. Im allgemeinen liegt eine gute Übereinstimmung zwischen Modellvoraussagen und Versuchsergebnissen vor.

## 1. INTRODUCTION

Knowledge of suitable constitutive equations is a necessary prerequisite for finite element ultimate load analysis of thick-walled structures made of reinforced concrete. During the last years a number of triaxial constitutive models, based on different mechanical concepts, have been proposed. So far, a comparative evaluation of their potential for modelling the behavior of concrete under multi-axial states of stress does not seem to exist in the open literature. This was the motivation for a comprehensive comparative study of a relatively large number of material laws proposed by several investigators to describe the mechanical behavior of concrete subjected to triaxial non-monotonic loading up to material failure [1].

The present paper is based on the mentioned investigation. It consists of a report on four constitutive models, selected from [1], representing four different mechanical concepts. The purpose of the paper is to provide information about the capability of typical representatives of different classes of constitutive models for description of the material behavior of multiaxially loaded concrete.

The chosen models are the Cauchy (nonlinear elastic) model by Kotsovos and Newman [2], the hypoelastic material law by Stankowski and Gerstle [3], an elasto-plastic constitutive model by Han and Chen [4] and a bounding surface model developed by the second author, reported in [1]. After description of these models a comparative evaluation is carried out. It is based on a comparison of results from selected load paths with corresponding test results.

## 2. CONSTITUTIVE MODELS

### 2.1 Cauchy (Nonlinear Elastic) Model by Kotsovos and Newman

This constitutive model is characterized by a total (secant) formulation. Introducing the octahedral strains, $\varepsilon_o = I_1'/3$ and $\gamma_o = \sqrt{2J_2'/3}$, and stresses, $\sigma_o = I_1/3$ and $\tau_o = \sqrt{2J_2/3}$, where $I_1$ is the first invariant of the stress tensor, $I_1'$ is the first invariant of the strain tensor, $J_2$ is the second invariant of the stress deviation tensor and $J_2'$ is the second invariant of the strain deviation tensor, the constitutive equations are given as [2]:

$$\varepsilon_o = (\sigma_o + \sigma_o')/(3K_S) \quad , \qquad \gamma_o = \tau_o/(2G_S) \quad . \tag{1}$$

The two secant material moduli, $K_S$ (bulk modulus) and $G_S$ (shear modulus), depend on the uniaxial compressive strength of concrete, $f_{cu}$. They are obtained by means of curve fitting, using experimental results. An essential feature of this constitutive model is the quantity [2]

$$\sigma_o' = f(\sigma_o, \tau_o) = \{a(\tau_o/f_{cu})^b\}/\{1+c(\sigma_o/f_{cu})^d\} \tag{2}$$

where a,b,c and d are regression coefficients. The purpose of adding $\sigma_o'$ to $\sigma_o$ in the expression for $\varepsilon_o$ is consideration of the fact that deviatoric loading yields deviatoric as well as volumetric deformations.

Recomputations of several experiments have shown that for the case of nonproportional loading the constitutive model by Kotsovos and Newman is deficient. The shortcomings are caused by (a) the lack of a parameter considering the load history (introduction of such a quantity, however, would be beyond the scope of a classical Cauchy model) and (b) the loading criterion based on the octahedral stresses. The second deficiency was eliminated by introducing a loading criterion proposed by Stankowski and Gerstle [3], which is based on the principal normal stresses. According to this criterion, loading in the direction of a principal normal stress $\sigma_i$ is characterized by exceeding the previously reached maximum

value of the respective principal normal stress.

Fig.1 illustrates the difference between the two criteria. For the considered stress path the first criterion indicates triaxial loading up to point O followed by hydrostatic unloading and deviatoric loading (Fig.1(a)). According to the second criterion, unloading in the directions of $\sigma_2$ and $\sigma_3$ begins already at point P (Fig.1(b)). This criterion agrees very well with test results.
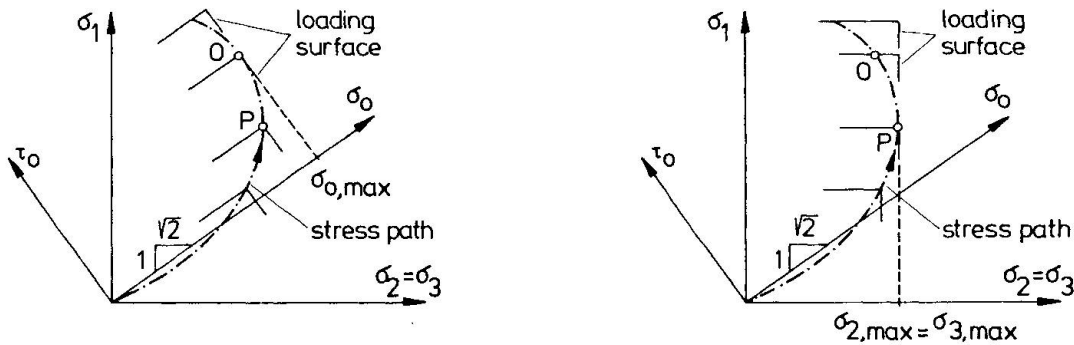
(a) octahedral stress criterion     (b) principal normal stress criterion

Fig.1 Loading Surfaces in the Stress Space for Two Different Loading Criteria

Determination of deformations resulting from nonmonotonic loading requires formulation of an incremental relationship $\Delta\epsilon = D_T\Delta\sigma$, where $D_T$ is a tangent material matrix relating increments of principal normal stresses to increments of principal normal strains. For a situation characterized by loading in the direction of $\sigma_1$ and unloading in the directions of $\sigma_2$ and $\sigma_3$, this relationship is given as

$$\begin{Bmatrix} \Delta\epsilon_1 \\ \Delta\epsilon_2 \\ \Delta\epsilon_3 \end{Bmatrix} = \begin{bmatrix} \alpha_1 & \beta & \beta \\ \beta & \alpha' & \beta' \\ \beta & \beta' & \alpha' \end{bmatrix} \begin{Bmatrix} \Delta\sigma_1 \\ \Delta\sigma_2 \\ \Delta\sigma_3 \end{Bmatrix} , \tag{3}$$

where

$$\begin{aligned} \alpha' &= 1/(9K_0)+1/(3G_0) , & \alpha_1 &= 1/(9K_T)+1/(3G_T)+\Delta\sigma_0'/(3K_T\Delta\sigma_1) \\ \beta' &= 1/(9K_0)-1/(6G_0) , & \beta &= 1/(9K_T)-1/(6G_T) \end{aligned} \tag{4}$$

The tangent material moduli $K_T$ and $G_T$ are obtained through differentiation of $K_S$ and $G_S$. The material behavior described by the Eqs.3 and 4 is called "transversely isotropic" [5]. It is characterized by material properties in the direction of $\sigma_1$ which are different from the ones in a plane normal to this direction, representing a plane of isotropy.

## 2.2 Hypoelastic Model by Stankowski and Gerstle

This nonlinear material model is characterized by an incremental (tangent) formulation. The respective constitutive equations are given as [3]

$$\begin{Bmatrix} \Delta\epsilon_0 \\ \Delta\gamma_0 \end{Bmatrix} = \begin{bmatrix} 1/(3K_T) & 1/H_T \\ 1/Y_T & 1/(2G_T) \end{bmatrix} \begin{Bmatrix} \Delta\sigma_0 \\ \Delta\tau_0 \end{Bmatrix} , \tag{5}$$

where $K_T = f(\sigma_0)$ and $G_T = f(\sigma_0,\tau_0)$ are obtained through curve fitting, using experimental results. The coupling tangent material moduli $H_T$ and $Y_T$ permit consideration of the influence of $\Delta\tau_0$ on $\Delta\epsilon_0$ and of $\Delta\sigma_0$ on $\Delta\gamma_0$, respectively. With regards to constitutive modelling of these interactions, Stankowski and Gerstle were influenced by results obtained by Scavuzzo et al. [6] from comprehensive test series.

For the current state of stress, characterized by point P on the stress path shown in Fig.2(a), $\Delta\epsilon_0^{pl}/\Delta\gamma_0^{pl} = 1/\sqrt{2}$ where $\Delta\epsilon_0^{pl}$ and $\Delta\gamma_0^{pl}$ are increments of the

plastic octahedral strains. Using the following relationships for a purely deviatoric load increment:

$$\Delta\epsilon_o = \Delta\epsilon_o^{el} + \Delta\epsilon_o^{pl} = 0 + \Delta\epsilon_o^{pl} = \Delta\tau_o/H_T \qquad \text{and} \qquad (6)$$

$$\Delta\gamma_o = \Delta\gamma_o^{el} + \Delta\gamma_o^{pl} = \Delta\tau_o/(2G_0) + \Delta\gamma_o^{pl} = \Delta\tau_o/(2G_T) \qquad (7)$$

where $\Delta\epsilon_o$ ($\Delta\epsilon_o^{el}$) and $\Delta\gamma$ ($\Delta\gamma_o^{el}$) are increments of the (elastic) octahedral strains, in order to express $\Delta\epsilon_o^{pl}/\Delta\gamma_o^{pl}$ in terms of $H_T$, $G_T$ and $G_0$, where $G_0$ is the initial value of G, and setting this expression equal to $1/\sqrt{2}$, yields

$$H_T = 2\sqrt{2}G_T/(1-G_T/G_0). \qquad (8)$$

Considering a purely volumetric load increment, by analogy to determination of $H_T$, $Y_T$ is obtained as

$$Y_T = 3K_T/\{\sqrt{2}(1-K_T/K_0)\} \qquad (9)$$

where $K_0$ is the initial value of K.



(a) increments of plastic strains  (b) corrective factor $F = f(\tau_o/\tau_{ou})$

Fig.2 Rotation of Vector $\Delta\epsilon^{pl}$ for Consideration of Volume Dilatation

According to the loading criterion based on the principal normal stresses, for purely deviatoric loading the loading surfaces are normal to the direction of $\sigma_1$. Thus, $\Delta\epsilon_o^{pl}>0$ (Fig.2(a)), indicating volume contraction irrespective of the magnitude of $\tau_o$. By contrast to this analytical result, it is known from experiments that a change from volume contraction to dilatation occurs when $\tau_o$ exceeds a value of approximately $0.9\tau_{ou}$ where $\tau_{ou}$ is the octahedral shear strength. In order to consider this fact, Stankowski and Gerstle have redefined the ratio $\Delta\epsilon_o^{pl}/\Delta\gamma_o^{pl}$ as $\Delta\epsilon_o^{pl}/\Delta\gamma_o^{pl} = F/\sqrt{2}$ where F is a corrective factor depending on $\tau_o/\tau_{ou}$ as shown in Fig.2(b). This factor results in a rotation of the vector $\Delta\epsilon^{pl}$ such that for $\tau_o = \tau_{ou}$ it is normal to the failure envelope. For negative values of F, $\Delta\epsilon_o^{pl}< 0$, indicating volume dilatation.

For axisymmetric states of stress, the two quantities $\Delta\epsilon_o$ and $\Delta\gamma_o$ are sufficient for determination of $\Delta\epsilon_1$ and $\Delta\epsilon_2 = \Delta\epsilon_3$. For general triaxial states of stress, however, an additional condition is necessary to determine $\Delta\epsilon_1$, $\Delta\epsilon_2$ and $\Delta\epsilon_3$ from $\Delta\epsilon_o$ and $\Delta\gamma_o$. It is assumed that the directions of the increments of the stress deviation vector coincide with the directions of the corresponding increments of the strain deviation vector. In general, however, this assumption does not agree with reality.

## 2.3 Elasto-Plastic Model by Han and Chen

The hardening characteristics of this constitutive model account for the ductility of concrete under compression and for its brittleness under tension. The loading surface expands from the (initial) yield surface to the failure surface (Fig.3(a)). It is described by the relationship [4]

$$f = r - kr_f(\sigma_m, \theta) = 0 \qquad (10)$$

where $r = \sqrt{2J_2}/f_{cu}$ is the deviatoric length normalized with respect to $f_{cu}$, $\sigma_m = \sigma_o/f_{cu}$, $\theta = (1/3)\arccos\left[(3\sqrt{3}/2)(J_3J_2^{(3/2)})\right]$ is the Lode angle with $J_3$ as the third invariant of the stress deviation tensor, $k$ is a form factor depending on $\sigma_m$ and on the hardening parameter $k_o$ characterized by $k_y \leq k_o \leq 1$, with $k_o = k_y$ and $k_o = 1$ referring to the yield surface and to the failure surface $r = r_f$, respectively. Results presented in this paper, which are based on the constitutive model by Han and Chen, were obtained by means of the failure surface by Willam and Warnke [7].



(a) expansion of the yield surface    (b) construction of a loading surface
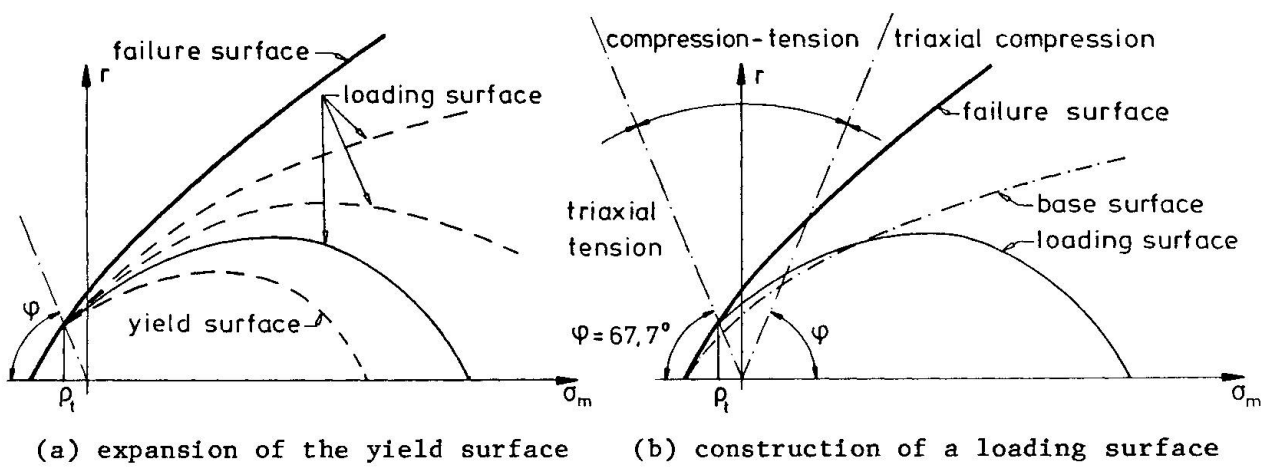
Fig.3 Expansion of the Yield Surface and Construction of a Loading Surface

The starting point for the construction of a loading surface is the base surface (Fig.3(b)), representing an affine contraction of the failure surface. It is described by the relationship

$$f_b = r - k_o r_f = 0. \qquad (11)$$

The shape function $k = k(\sigma_m, k_o)$, defining the corresponding loading surface, is determined such that for triaxial tension $(\sigma_m \geq \rho_t)$ there is no hardening zone (Fig.3). Additional aspects for determination of $k$ are the increase of the hardening zone with increasing hydrostatic compression and the close up of the loading surface at the hydrostatic axis in the region of triaxial compression, indicating a large hardening zone.

The hardening parameter $k_o$ is determined with the help of a $\sigma$-$\varepsilon^{pl}$ diagram where $\sigma$ and $\varepsilon^{pl}$ are the stress and the plastic strain, respectively, obtained from a uniaxial compression test, and of the condition

$$dW^{pl} = \sigma_{ij}d\varepsilon_{ij}^{pl} = \sigma d\varepsilon^{pl} \qquad (12)$$

where $dW^{pl}$ is a differential of the specific plastic work and $d\varepsilon_{ij}^{pl}$ is a differential of the plastic strains $\varepsilon_{ij}^{pl}$. Thus, each loading surface is associated with a so-called base plastic modulus $H_b^{pl} = d\sigma/d\varepsilon^{pl}$, resulting from the uniaxial compression test [4].

In order to consider the ductile material behavior of concrete under triaxial

compression, $H_b^{pl}$ was replaced by a modified plastic modulus $H^{pl} = M(\sigma_m,\theta) \cdot H_b^{pl}$ where M is a modification factor. For large compressive stresses the form of M suggested by Han and Chen [4] yields a physically unrealistic restiffening of the material.

For the purpose of an adequate description of volume contraction and dilatancy, the direction of the vector of plastic flow is defined by a nonassociated flow rule which can be written formally as

$$d\epsilon_{ij}^{pl} = d\lambda \partial g/\partial \sigma_{ij} \tag{13}$$

where $d\lambda$ is a positive scalar factor of proportionality and g is the plastic potential given as [4]

$$g = \alpha I_1 + \sqrt{J_2} - k* = 0 \tag{14}$$

where $\alpha$ represents the plastic dilatancy factor, proposed in [4] as a linear function of $k_o$, and k* is a constant which does not appear in the flow rule. The dilatancy factor controls the description of the $\tau_o - \epsilon_o^{pl}$ relationship. It also has an influence on the stiffness modulus h, appearing in the expression for the plastic material stiffness tensor (Eq.16).

A shortcoming of the original form of $\alpha = \alpha(k_o)$, which occurs when leaving the hydrostatic axis after a significant elasto-plastic hydrostatic preloading, is the strong rotation of the vector of plastic flow $d\epsilon_{ij}^{pl}$ in the direction of the $\tau_o$-axis, connected with a considerable decrease of $(\partial g/\partial \sigma_{ij})\sigma_{ij}$ and, thus, of h (Eq.17). Thus, a modified dilatancy factor $\alpha(k,k_o,k_y,f_{cu},\theta,\sigma_o)$ was used in the numerical investigation for the present paper. This factor is based on test results showing the dependence of the $\tau_o - \epsilon_o^{pl}$ relationship on $f_{cu}$, $\theta$, and $\sigma_m$ and on the type of loading.

The incremental stress-strain equations can be written formally as

$$d\sigma_{ij} = (D_{ijkl}^{el} + D_{ijkl}^{pl}) \, d\epsilon_{kl} \tag{15}$$

where $D_{ijkl}^{el}$ is the elastic and $D_{ijkl}^{pl}$ is the (unsymmetric) plastic material stiffness tensor, given as [4]

$$D_{ijkl}^{pl} = -(1/h)\left(D_{ijmn}^{el}(\partial g/\partial \sigma_{mn})(\partial f/\partial \sigma_{pq})D_{pqkl}^{el}\right) \tag{16}$$

with

$$h = (\partial f/\partial \sigma_{mn})D_{mnpq}^{el}(\partial g/\partial \sigma_{pq}) - H^{pl}(\partial f/\partial \sigma)(1/\sigma)(\partial g/\partial \sigma_{ij})\sigma_{ij}. \tag{17}$$

## 2.4 Bounding Surface Model by Meschke

This constitutive model belongs to a special category of bounding surface models, characterized by the vanishing of the elastic range. The mathematical formulation of such bounding surface models was introduced first by Dafalias and Popov [8]. The constitutive model proposed by Meschke [1] is based on the concept of hypo-plasticity. According to Dafalias [9], the main distinguishing factor of hypo-plasticity from ordinary plasticity is the dependence of the plastic strain rate and of the rate of the internal variables on the stress rate direction, in addition to the overall dependence on the stress state. Thus, for nonproportional loading hypoplasticity is incrementally nonlinear.

The basic relationship of the bounding surface model by Meschke is the equation

$$d\epsilon^{pl} = (1/H^{pl})<L>\rho \tag{18}$$

where $\varepsilon^{pl}$ is the vector of plastic flow, $H^{pl} = H^{pl}(\sigma,k,\varepsilon^{pl})$ is a generalized plastic modulus, $<L>$ is a loading function defined as $<L> = L = d\sigma.n$ for $d\sigma.n > 0$ and as $<L> = 0$ for $d\sigma.n \leq 0$ with $n$ representing the normal vector at the image stress point $\sigma_b$ on the loading surface (Fig.4), and $\rho$ is a direction vector given as $\rho = d\varepsilon^{pl}/|d\varepsilon^{pl}|$. $H^{pl}$ depends on the stress vector $\sigma$, defining a point in the space of principal stresses $\sigma_i$, on the normalized distance parameter $k = k(r,r_f,\xi)$, where $\xi$ is a discrete internal variable representing a jump parameter which accounts for abrupt changes of the loading direction, and on the accumulated effective plastic strain $\varepsilon^{pl}$, representing an internal variable, given as

$$\varepsilon^{pl} = \int d\varepsilon^{pl} = \int (d\varepsilon^{pl}.d\varepsilon^{pl})^{1/2}. \tag{19}$$

With the help of Eq.(18) and of the relationship $d\varepsilon = d\varepsilon^{el} + d\varepsilon^{pl}$ where $d\varepsilon$ and $d\varepsilon^{el}$ correspond to $d\varepsilon_{ij}$ and $d\varepsilon_{ij}^{el}$, respectively, the bounding surface model by Meschke can be formulated mathematically as follows:

$$d\sigma = D^{ep}d\varepsilon = \left(D^{el} - (D^{el}\rho \ D^{el}n)/(n \ D^{el}\rho + H^{pl})\right)d\varepsilon \tag{20}$$

where $D^{ep} = D^{el} + D^{pl}$ is the elasto-plastic material stiffness matrix with $D^{el}$ as the elastic and $D^{pl}$ as the plastic material stiffness matrix.

Fig.4 illustrates a meridional section of the bounding surface, which is identical to the failure envelope, at two different levels of deviatoric loading, indicated by the stress point $\sigma$. A comparison of the two illustrations shows the rotation of the direction vector during deviatoric loading. The point designated as $\sigma_{2,max} = \sigma_{3,max}$ refers to the maximum value of the respective principal normal stress.
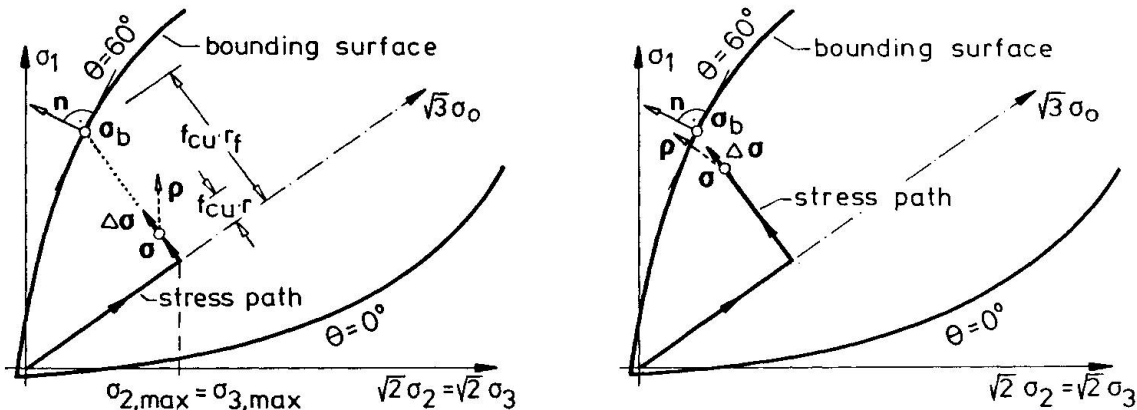


Fig.4 Rotation of the Direction Vector $\rho$ in the Course of Deviatoric Loading

The following list refers to characteristics of the proposed bounding surface model:

(a) The loading surface degenerates to the actual stress point.

(b) Using the projection rule by Mróz [8], the gradient of the loading surface is replaced by the gradient $n$ of the bounding surface $F(\sigma) = r - r_f = 0$ at the stress image point $\sigma_b$ (Fig.4). In the pre-failure material regime the bounding surface is fixed in the stress space. At present, the post-failure behavior of the material is not considered.

(c) The direction vector $\rho$ which controls the direction of the vector $d\varepsilon^{pl}$ is determined on the basis of experimental results reported by Scavuzzo et al. [6]. For a stress point at a sufficiently large distance from the failure envelope, the direction of the largest principal stress reached so far in the

process of loading controls the direction of $\rho$. (With regards to Fig.4, this is the $\sigma_1$-direction). As the stress point approaches the failure surface, the direction vector $\rho$ rotates towards the direction of the gradient vector **n**. This rotation is controlled by the distance parameter k. Abrupt changes of the direction of $\Delta\sigma$, as occur, e.g., for unloading, are considered by means of the jump parameter $\xi$. For proportional loading, $\xi = 0$ and $k = r/r_f$.

(d) With increasing tension the rotation of $\rho$ becomes slower.

(e) The value of the generalized plastic modulus $H^{pl}$ is controlled by $\sigma$, k, $\epsilon^{pl}$ and, because of $k = k(\xi)$, by the jump parameter $\xi$. Based on the stability criterion by Drucker, a lower bound of $H^{pl}$ is obtained as

$$H_S^{pl} = -(1/2)n\ D^{el}\rho + (1/2)\{(\rho\ D^{el}\rho)(n\ Dn)\}^{1/2}.$$

(21)

$H_S^{pl}$ depends on the amount of the rotation of $d\epsilon^{pl}$ in the course of loading up to failure. The effectiveness of this bound depends on the stress path.

(f) The loading criterion by Stankowski and Gerstle [3] is used.


## 3. COMPARATIVE EVALUATION OF THE SELECTED CONSTITUTIVE MODELS

The following comparative evaluation is based on four different loading paths. They were chosen such that the capability of the different formulations to describe specific characteristics of concrete subjected to nonproportional and nonmonotonic loading can be investigated.

Fig.5 shows $\tau_o/f_{cu}-\epsilon_o$ diagrams for purely deviatoric loading at two different hydrostatic load levels. The symbol "x" in Fig.5 refers to material failure. The test results illustrate the characteristic volumetric deformational behavior of concrete. Fig.5 elucidates that the nonlinear elastic constitutive model by Kotsovos and Newman does not account for dilatancy. The results obtained by the hypoelastic constitutive model of Stankowski and Gerstle are reasonably good. However, for loading path (b), this model underestimates the ultimate strength of the material by approximately 10 %. With regards to the elasto-plastic constitutive model by Han and Chen, for high hydrostatic load levels such as for loading path (b), the slope of the $\tau_o/f_{cu}-\epsilon_o$ diagram at the beginning of deviatoric loading is too small. The reason for this shortcoming is the acute angle enclosed by the hydrostatic axis and the loading surface at the apex of the latter. The good correlation of the compaction/dilatancy characteristics is the result of the previously mentioned modification of the original dilatancy factor $\alpha$. The constitutive model by Meschke yields results which agree reasonably well with the test results.

Fig.6 shows $\sigma_o/f_{cu}-\gamma_o$ diagrams for hydrostatic loading and unloading at different deviatoric load levels. The analytical results in Fig.6 obtained by the two nonlinear elastic constitutive models and by the hypoplastic material model by Meschke, respectively, satisfy the principal stress loading criterion. At point A of loading path (a) at which the principal stress $\sigma_1$ exceeds the largest previously obtained value, the beginning of virgin loading is signalled. For this loading path and for the chosen loading surface the loading criterion of the theory of plasticity, used by Han and Chen for their elasto-plastic constitutive model, happens to be equally good as the principal stress loading criterion. For loading path (b), however, the loading criterion of the theory of plasticity results in a delayed beginning of the deviatoric plastic deformations. For this loading path all constitutive models underestimate the octahedral shear strain $\gamma_o$. As far as the nonlinear elastic material models are concerned, disregard of the dependence of the tangent bulk modulus $K_T$ on $\tau_o$ appears to be the reason for this underestimation. The hypoplastic formulation by Meschke is found to be cap-
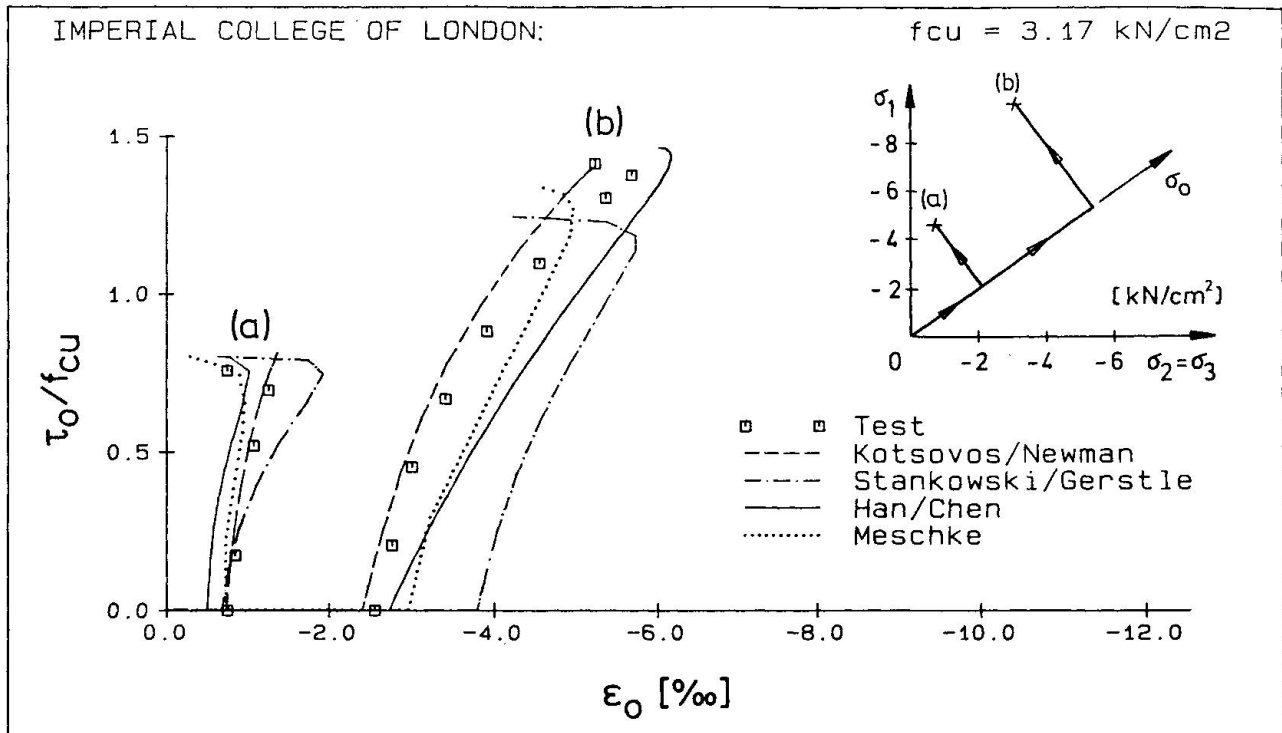
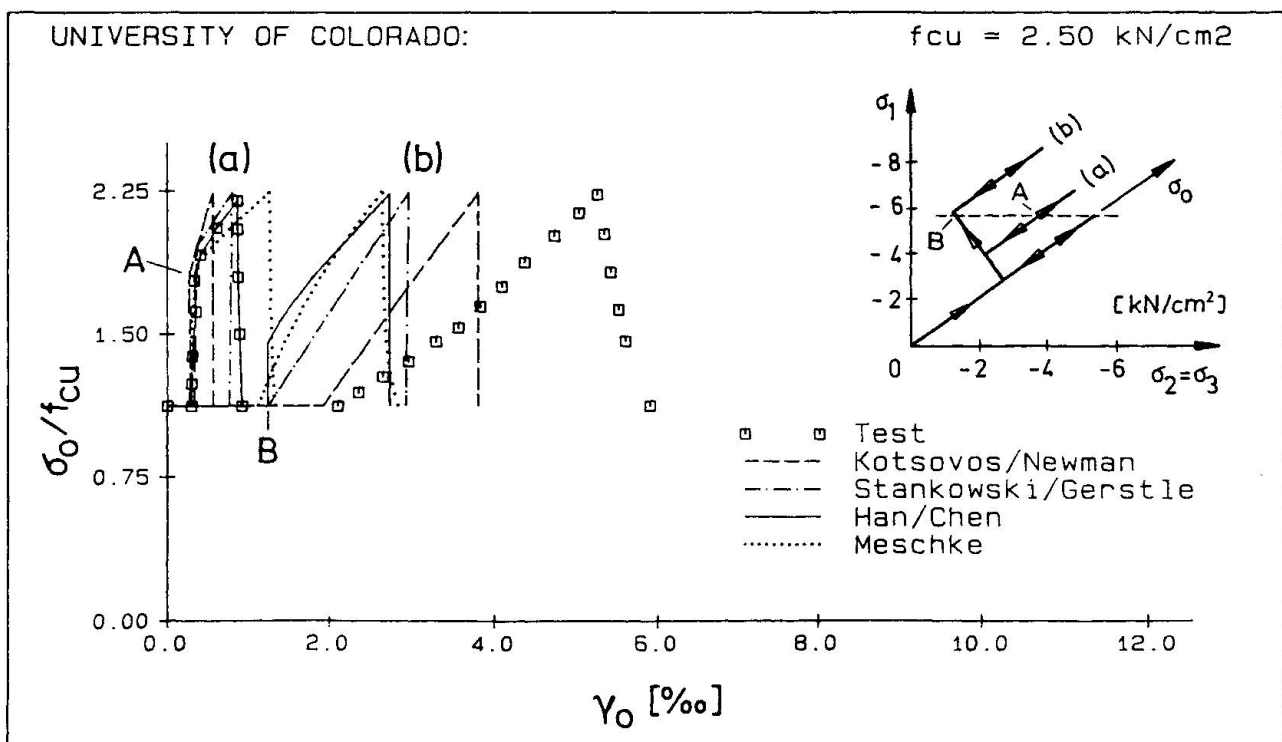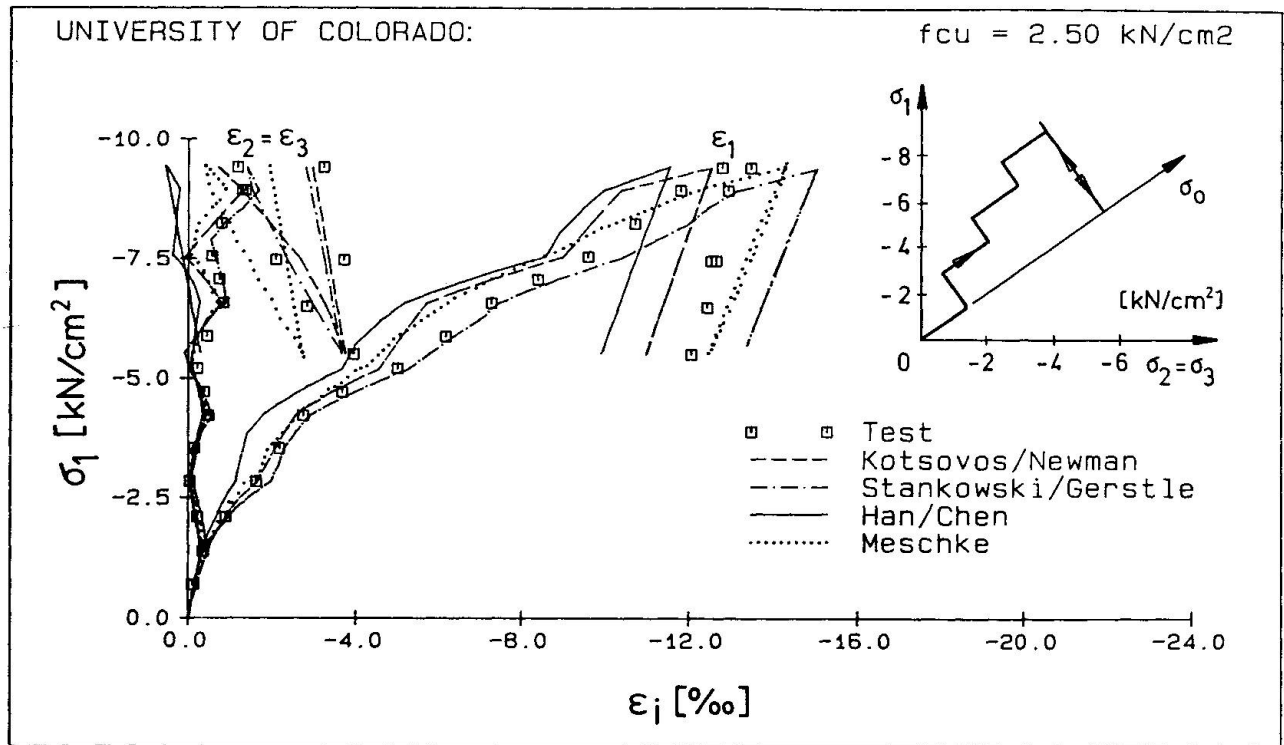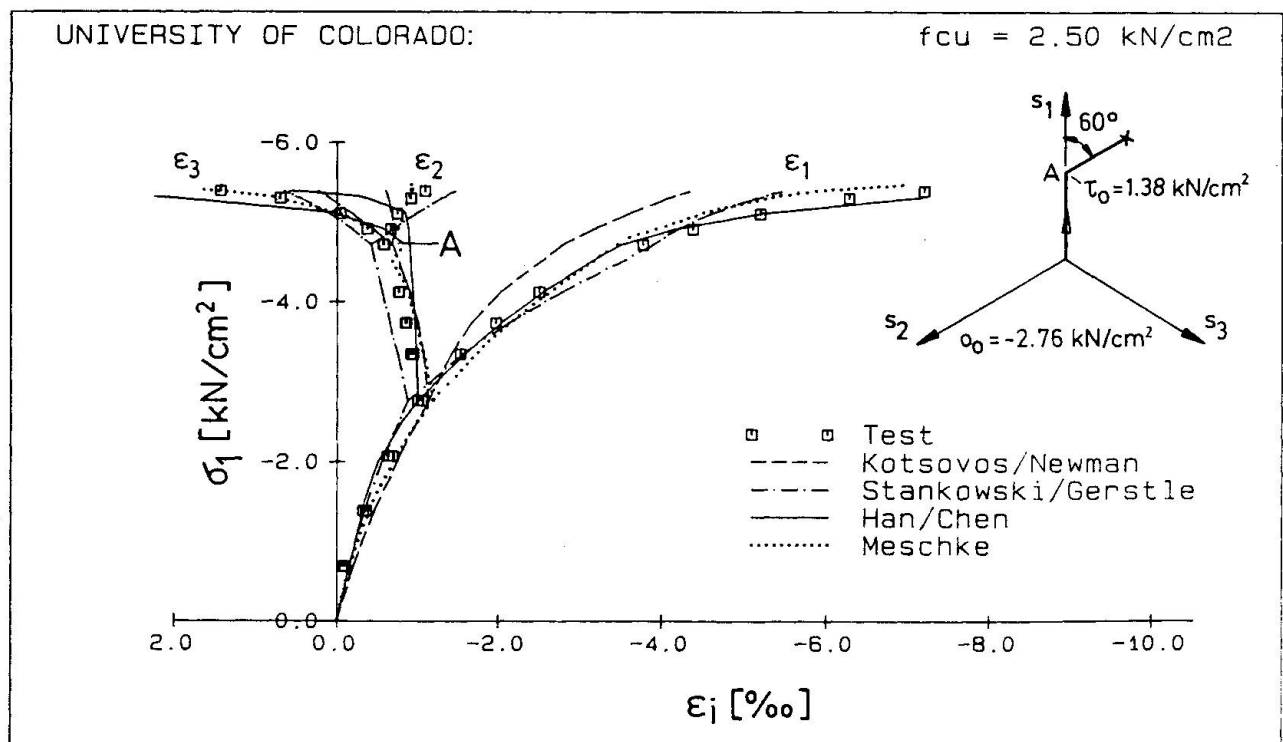Fig.5 Deviatoric Loading at Two Different Hydrostatic Load Levels



Fig.6 Hydrostatic Loading and Unloading at Different Deviatoric Load Levels

**Fig.7** Alternating Hydrostatic and Deviatoric Load Steps Followed by Deviatoric Unloading and Reloading



**Fig.8** Nonproportional Deviatoric Load Path after Hydrostatic Preloading

able of modelling the remarkable increase of $\gamma_0$ during hydrostatic unloading.

Fig.7 shows $\sigma_1$-$\varepsilon_i$ diagrams for a load history characterized by alternating hydrostatic and deviatoric load steps followed by deviatoric unloading and reloading. At points referring to changes from one of these two kinds of load steps to the other one the curves obtained by the constitutive model by Han and Chen are not smooth which is typical for elasto-plastic formulations. The linear elastic unloading predicted by the constitutive model by Han and Chen does not agree with the test results which show a considerable increase of plastic strains $\varepsilon_2^{pl}$ and $\varepsilon_3^{pl}$. This shortcoming of the material model by Han and Chen is attributed to the use of the loading criterion of the theory of plasticity. This underlines the importance of the principal normal stress criterion.

Fig.8 shows $\sigma_1$-$\varepsilon_i$ diagrams for a load history characterized by a nonproportional deviatoric load path after hydrostatic preloading. The symbol "x" in Fig.8 refers to material failure. The reason for the difference between the test results and the analytical results obtained from the formulation of Kotsovos and Newman is disregard of the dependence of the tangent bulk modulus $K_T$ on $\tau_0$. For the section of the deviatoric load path beginning at point A ($\sigma_0$ = -2.76 kN/cm$^2$, $\tau_0$ = 1.38 kN/cm$^2$) on the projection $s_1$ of the $\sigma_1$-axis onto the deviatoric plane, the elasto-plastic material model by Han and Chen yields incorrect strains $\varepsilon_2$. The reason for this shortcoming is the assumption of a circular shape of the section of the plastic potential surface by the considered deviatoric plane. For the hypoplastic constitutive model by Meschke good agreement between analytic and test results is observed.

## 4. CONCLUSIONS

Despite different mechanical concepts of the selected constitutive models and the fact that not all shortcomings inherent in some of these models could be eliminated, generally, good agreement between the model predictions of the deformational behavior and the ultimate strength of concrete and the test results was found. This also refers to results for the tension-compression material regime, which were not presented in this paper. At present, these material models are implemented in a multi-purpose finite element program.

Stress paths associated with characteristic points of thick-walled structures made of reinforced concrete, subjected to static loading, usually are less complex than the ones investigated in this paper. Therefore, for identical constitutive modelling of the post-failure behavior of concrete, it is expected that the chosen constitutive models for triaxially loaded concrete do not have much influence on the results of finite element ultimate load analysis of such structures.

## ACKNOWLEDGEMENT

## REFERENCES

1. EBERHARDSTEINER J., MESCHKE G. and MANG H.A., Triaxiales konstitutives Modellieren von Beton zum Zwecke der Durchführung vergleichender Traglastanalysen dickwandiger Stahlbetonkonstruktionen mittels der Methode der Finiten Elemente, Report, Institute for Strength of Materials, Technical University of Vienna, Vienna, 1987.

2. KOTSOVOS M.D., Concrete. A Brittle Fracturing Material, Material and Struc-
tures, RILEM, Vol.17, No.98, 1984.

3. STANKOWSKI T. and GERSTLE K.H., Simple Formulation of Concrete Behavior under
Multiaxial Load Histories, Journal of the American Concrete Institute, Vol.82,
No.2, 1985.

4. HAN D.J., CHEN W.F., A Nonuniform Hardening Plasticity Model for Concrete
Materials, Mechanics of Materials, No.4, 1985.

5. CHEN W.F. and SALEEB A.F., Constitutive Equations for Engineering Materials,
Vol.1, Elasticity and Modeling, Wiley, New York, 1981.

6. SCAVUZZO R., STANKOWSKI T., GERSTLE K.H. and KO H.Y., Stress-Strain Curves
under Multiaxial Load Histories, Report, Dept. of Civil, Environmental and
Architectural Engineering, University of Colorado, Boulder, USA, August 1983.

7. WILLAM K.J. and WARNKE E.P., Constitutive Model for the Triaxial Behavior of
Concrete, International Association for Bridge and Structural Engineering,
Seminar on Concrete Structures Subjected to Triaxial Stresses, No.III-1, Ber-
gamo, Italy, 1974.

8. DAFALIAS Y.F, POPOV E.P., Cyclic Loading for Materials with a Vanishing Elas-
tic Region, Nuclear Engineering and Design, Vol.41, 1977.

9. DAFALIAS Y.F., Bounding Surface Plasticity. I: Mathematical Foundation and
Hypoplasticity, Proceedings of the ASCE, Journal of the Engineering Mechanics
Division, Vol.112, EM9, 1986.